MODELLING VERTICAL VARIATION OF TURBULENT FLOW ACROSS A SURF ZONE USING SWASH

Marcel Zijlema[1]

This paper presents the application of the open source non-hydrostatic wave-flow model SWASH to propagation of irregular waves in a barred surf zone, and the model results are discussed by comparing against an extensive laboratory data set. This study focus not only on wave transformation in the surf zone, but also on the numerical prediction of undertow and vertical distribution of turbulence levels under broken waves. Present simulations demonstrate the overall predictive capabilities of the model in computing breaking surf zone waves.

Keywords: surf zone; wave breaking; undertow; turbulence modelling; SWASH

INTRODUCTION

The prediction of the wave characteristics and vertical flow structures in the surf zone is an active area of research and is of utmost importance to many disciplines within coastal engineering. In the surf zone, the flow is highly rotational, where wave breaking and turbulence play an important role. Under breaking waves, the level of wave-induced current in the water column is mainly dictated by the balance between the cross-shore gradient of the radiation stress and the pressure gradient due to wave set-up. However, while the pressure gradient is nearly uniform over the depth, the radiation stress gradient is highest near the free surface from where it decreases to the bed. As a consequence, the resulted wave-averaged current is directed seaward near the bed and onshore-directed higher in the water column. In addition, this vertical undertow profile is affected by breaking induced turbulence, particularly near the surface, which enhances the mixing of momentum. The undertow also interacts with the bed characterising a wave-current boundary layer, while exchanging momentum due to shear-generated turbulence.

Not surprisingly, many numerical models have been discussed in the literature, as they provide details of the flow without scaling difficulties. Two types of numerical models for the simulation of flow and waves in the surf zone can be distinguished: wave-averaged models and phase-resolving wave models. These models are able to predict the amount of undertow fairly well. For an overview, see Christensen et al. (2002). The first type usually simulates waves and currents separately, while their interaction is based on data coupling. Wave-current interaction is thus obtained through repetitively execution of the flow module followed by the wave module. Furthermore, wave-averaged models contain a number of free but unknown parameters (e.g. the wave breaking criterion) that requires a rather extensive calibration. Examples of this type of modelling can be found in Wenneker et al. (2011) and Van der Werf et al. (2013). On the other hand, phase-resolving models are, in principle, able to take into account the wave-current interaction and wave breaking directly. A good example is a quantitative study of Lin and Liu (1998) with their VOF model applied to the surf zone. Other examples are Bradford (2000), Zhao et al. (2004) and Wang et al. (2009).

In this paper, we investigate the applicability of a more efficient non-hydrostatic wave-flow model, since it allows to simulate large basins in a practical length of computational time. Particularly, we simulate the surf zone dynamics across a barred beach, under controlled laboratory conditions, by means of the SWASH model as described in Zijlema et al. (2011). We focus mainly on the vertical distribution of time-averaged horizontal velocity and turbulent kinetic energy.

SWASH: A NON-HYDROSTATIC WAVE-FLOW MODEL

Introduction

Non-hydrostatic wave-flow models are gaining recognition as to be evolved out of a wish to achieve a compromise between the capabilities of the Boussinesq-type wave models and operational-based requirements for numerical robustness, simplicity, ease of use and economy. These models are still being explored, refined and validated but are likely to remain the most appropriate route to simulate surf zone dynamics for some years to come. Over the past ten years, strong efforts have been made at Delft University to advance the state of wave modelling and flooding simulations for coastal engineering applications. These efforts have focused on developing and validating the newly developed non-hydrostatic wave-flow model SWASH

[1]Environmental Fluid Mechanics Section, Faculty of Civil Engineering and Geosciences, Delft University of Technology, P.O. Box 5048, 2600 GA Delft, The Netherlands

Zijlema et al. (2011). This open source code (http://swash.sourceforge.net) is intended to be used for predicting transformation of surface waves and rapidly varied shallow water flows in coastal waters. SWASH is capable of simulating the flow at any scale giving very detailed information, while it often does not require any calibration.

Numerical framework

SWASH (an acronym of Simulating WAves till SHore) takes as its starting point the Reynolds-averaged Navier-Stokes equations for the computation of the surface elevation and currents in incompressible flow. As a matter of fact, these equations can be regarded as nonlinear shallow water (NLSW) equations including the effect of vertical acceleration. For the present purpose of outlining the principles adopted, the precise form of the governing equations is irrelevant. However, one is refer to Zijlema and Stelling (2005) and Zijlema et al. (2011) for details. Also, details on the imposition of the boundary conditions can be found in, e.g. Rijnsdorp et al. (2014). In this section, a brief outline of some numerical procedures relevant to the surf zone applications is given.

SWASH employs an explicit, second order finite difference method for staggered grids. This framework is the most natural and advantageous basis for advanced wave modelling in coastal areas. For accuracy reason, the pressure is split-up into hydrostatic and non-hydrostatic parts. Moreover, space discretization precedes introduction of pressure correction, so that no artificial pressure boundary conditions are required. Horizontal advection terms in the momentum equations are approximated by means of central differences, while a first order upwind scheme is employed for the vertical advection terms.

To ease the task of discretization and to enhance the accuracy of the scheme, a vertical boundary-fitted co-ordinate system is employed, permitting more resolution near the bottom as well as near the free surface. This co-ordinate change allows a number of layers having a relative thickness, i.e. a percentage of the local water depth, or uniform constant thickness for each layer. Space discretization in the vertical direction is carried out in a finite volume fashion. For details, see Zijlema and Stelling (2005).

A discretized form of the NLSW equations can automatically be shock-capturing if the momentum conservation is retained in the finite difference scheme. The principle of this approach, as well as its underlying rationale are documented in Stelling and Duinmeijer (2003) and Zijlema and Stelling (2008). Given a sufficient number of vertical layers (10 or more), the adopted momentum-conservative scheme is able to track the actual location of incipient wave breaking accurately, without the need of empirical parameterization. The bore-like wave front steepens continuously until it becomes vertical. Subsequently, the broken wave propagates with a correct gradual change of form and resembles a steady bore in a final stage. This leads to a correct amount of energy dissipation on the front face of the breaking wave. As a matter of fact, this breaking wave can be regarded as a discontinuity in the flow variables (free surface and velocities) of which its proper numerical treatment, i.e. conservation of mass and momentum, is the basic foundation for capturing the integral properties of the breaking wave, like the jump height and the rate of energy dissipation. Also, intra-phase properties such as asymmetry and skewness are preserved as well.

With respect to time integration of the continuity and horizontal momentum equations, a second order leapfrog scheme, known as the Hansen scheme, is adopted so that the wave amplitude will not altered. A MacCormack predictor-corrector technique is employed in order to retain second order accuracy in time for the horizontal advection terms in the horizontal momentum equations. In addition, the vertical advection and viscosity terms are integrated in time using the semi-implicit $\theta-$method, which is a weighted average between first order explicit and implicit Euler schemes. In this study, we have chosen the second order accurate Crank-Nicolson scheme ($\theta = 0.5$).

Local mass continuity is enforced by solving a Poisson equation for the pressure correction which steers the non-hydrostatic pressure towards a state at which all mass residuals in the active grid cells become negligible small, reflecting a satisfaction of local mass conservation. The iterative solution of the unsymmetric Poisson equation for pressure correction is the most time consuming part and therefore, the efficient BiCGSTAB method accelerated with incomplete LU type preconditioners is employed. Global mass conservation is obtained by solving a depth-averaged continuity equation for the solution of the surface elevation.

Finally, a very simple wet-dry approach as treated in Stelling and Duinmeijer (2003) is adopted. This method tracks the motion of the shoreline very accurately without posing numerical instabilities by ensuring non-negative water depths and using the upwind water depths in the momentum flux approximations.

Turbulence modelling

The usual approach for simulating turbulent flow is the application of a turbulence model to close the Reynolds-averaged momentum equations. A still widely employed turbulence model is the $k-\varepsilon$ model of Launder and Spalding (1974), which is adopted in this study. Generally, in the surf zone, the horizontal length scales are relatively larger than the vertical ones and so, the vertical transport mechanism is dominant while the role of the horizontal transport is moderate; see also Lin and Liu (1998). Thus, we consider the Reynolds stress $-\overline{u'\,w'}$ which is related to the vertical mean rate of strain through the eddy viscosity, as follows

$$-\overline{u'\,w'} = \nu_v \frac{\partial u}{\partial z} \tag{1}$$

and the eddy viscosity is given by

$$\nu_v = c_\mu \frac{k^2}{\varepsilon} \tag{2}$$

with k the turbulent kinetic energy and ε the dissipation rate of turbulent energy. These turbulent quantities are governed by the following transport equations

$$\frac{\partial k}{\partial t} + u\frac{\partial k}{\partial x} + v\frac{\partial k}{\partial y} + \omega\frac{\partial k}{\partial z} = \frac{\partial}{\partial z}\left(\frac{\nu_v}{\sigma_k}\frac{\partial k}{\partial z}\right) + P_k - \varepsilon \tag{3}$$

and

$$\frac{\partial \varepsilon}{\partial t} + u\frac{\partial \varepsilon}{\partial x} + v\frac{\partial \varepsilon}{\partial y} + \omega\frac{\partial \varepsilon}{\partial z} = \frac{\partial}{\partial z}\left(\frac{\nu_v}{\sigma_\varepsilon}\frac{\partial \varepsilon}{\partial z}\right) + \frac{\varepsilon}{k}\left[c_{\varepsilon 1}P_k - c_{\varepsilon 2}\varepsilon\right] \tag{4}$$

where u and v are the horizontal velocities in cross-shore/x and longshore/y direction, respectively, ω is the vertical velocity oriented orthogonal to the vertical layer interfaces, and P_k is the production of turbulent energy due to mean shear, given by

$$P_k = \nu_v\left[\left(\frac{\partial u}{\partial z}\right)^2 + \left(\frac{\partial v}{\partial z}\right)^2\right] \tag{5}$$

Here, the horizontal velocity gradients as usually occur in the production term, Eq. 5, and the horizontal diffusivity terms in Eqs. 3 and 4 have been neglected.

The empirical coefficients c_μ, $c_{\varepsilon 1}$, $c_{\varepsilon 2}$, σ_k and σ_ε are dimensionless constants which, respectively, are taken to be 0.09, 1.44, 1.92, 1.0 and 1.3, as recommended in Launder and Spalding (1974). The values of these closure constants are obtained from experiments for local equilibrium shear layer and isotropic turbulence. Hence, these values remain unsure when applying to a wave-induced oscillatory boundary layer.

Lastly, wall functions based on the logarithmic wall-law are adopted near the bed to avoid compute-intensive integration through the viscous sublayer and to obtain log-layer solutions. Details can be found in Launder (1982). Either a smooth or rough bed can be considered. This represents a bottom boundary layer due to bed shear.

In SWASH, the equations for k and ε are treated as decoupled equations, in the following way: for each time step first the $k-$equation is solve using the updated velocities and non-updated turbulent quantities. The same holds for the equation for ε, which is solved after k. Both equations are integrated with a fractional step method. Each time step consists of two steps. In the first step, each transport equation to be solved is decoupled in the vertical and only the horizontal advection terms are updated. For reasons of robustness, these terms are approximated by means of a first order upwind scheme. In many cases this is accurate enough. In the second step, the same equation is decoupled in the horizontal, while the remaining terms, like vertical transport, production and dissipation rate, are treated. This treatment is such that k and ε are non-negative during the whole time step. In both steps the decoupled parts of the usually stiff turbulence equation are integrated in time fully implicitly, i.e. $\theta = 1$. The resulting systems of equations are solved using a Gauss-Seidel iterative technique and a Gaussian elimination, respectively.

LABORATORY TEST CASES

Boers (2005) carried out very detailed surface elevation and vertical velocity measurements in the wave flume of Delft University of Technology. The bed profile was based on a natural beach and included two breaker bars with a trough in between; see Fig. 1.

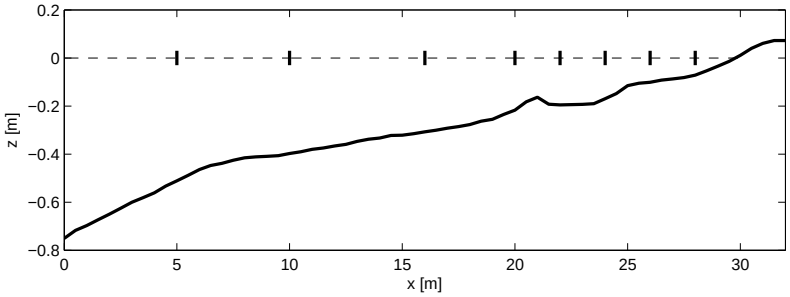

Figure 1: Bottom topography and location of gauges of the experiment of Boers (2005).

In this study we consider data from two irregular wave conditions, characterising a spilling breaker (1B) and a weakly plunging breaker (1C), respectively; see Table 1 (ξ is the surf similarity parameter). In these laboratory experiments, an extensively detailed measurements of the surf zone hydrodynamics were reported in Boers (2005). Vertical flow structures, like undertow and turbulent kinetic energy, at different locations in the surf zone (see Fig. 1), with typically 10 data points distributed over the depth, were measured as well. They will be used for the validation of SWASH to demonstrate the ability of the model to describe the turbulent flow at the presence of breaking waves across the surf zone.

Table 1: Measured wave conditions in the flume of Boers (2005) at the wavemaker.

case	H_{m0} [cm]	T_p [s]	ξ
1B	20.6	2.03	0.31
1C	10.3	3.33	0.71

MODEL SETUP

The considered cases were simulated with SWASH using the following settings. The calculations were run in the 2DV mode with a 0.02 m grid resolution in the horizontal direction and 20 equally distributed vertical layers. The time step was initially 0.001 s, while the maximum Courant number was 0.5. The simulations were long enough to get steady-state solutions. The bed was considered to be rough with a Nikuradse roughness length of 5 mm. No calibration nor tuning had been carried out in the course of simulations.

It should be noted that in the model the turbulent motions generated by wave breaking ("rollers") are not accounted for. The effect of this wave-induced turbulence on the vertical flow profiles is still not understood adequately; see also Boers (2005). In this study, it is assumed that the diffusive transport of wave-generated turbulence into the water column is negligble. As a consquence, the turbulence production resulted from (bed) shear remains dominant in the water column. The next section discuss how well this assumption holds by means of an analysis of the vertical variation of the flow across the surf zone.

RESULTS AND DISCUSSION

Case 1C

This case is characterized with a relatively low wave steepness while waves break in the shallow region only. In Fig. 2, spectral comparisons with the numerical and laboratory data are made. The spatial evolution of the wave spectra is represented by an amplification of spectral levels at both subharmonic and superharmonic ranges, consistent with three-wave interaction rules, followed by a transformation toward a broad spectral shape in the surf zone, attributed to the nonlinear couplings and wave energy dissipation. The model captures the dominant features of the attendant spectral evolution, both in the shoaling region and the surf zone. In terms of the wave height and wave setup, Fig. 3 shows that the quantitative trends are much well resolved by the model. Clearly, a strong and localized dissipation of energy has been taken place around the bars. The model prediction of both the onset of the breaking process and the amount of energy dissipation is excellent.

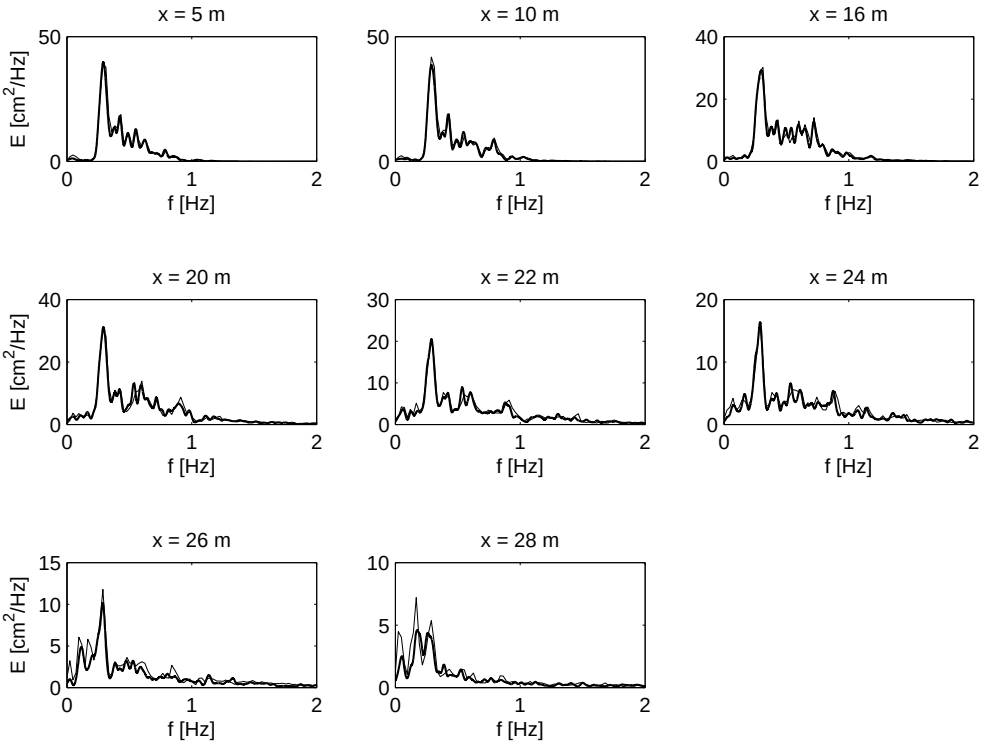

Figure 2: Predicted (thick line) and observed (thin line) energy density spectra at various wave locations for Boers 1C.

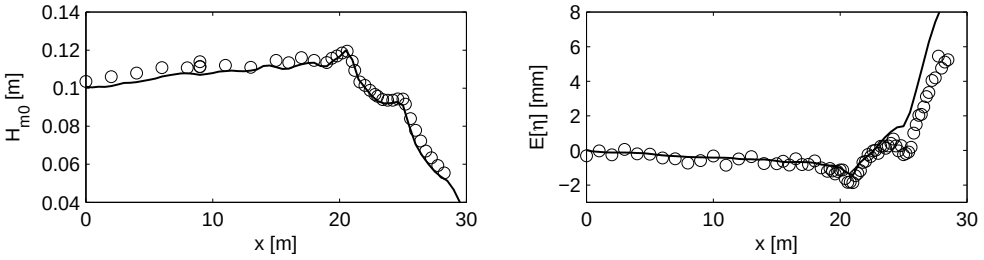

Figure 3: Computed and measured significant wave heights (left panel) and wave setup (right panel) along the flume for Boers 1C. Circles: experimental data; solid line: SWASH.

Fig. 4 presents a comparison of computed and measured wave-averaged horizontal velocity at different cross-shore locations. For the interpretation, we make a distinction between three different regions in the surf zone: offshore of the first breaker bar, i.e. $x < 22$ m, in between the first and second bar, i.e. $22 \leq x < 25$ m, and onshore of the second bar, i.e. $x \geq 25$ m. In general, the model is capable of simulating the deformation of the velocity profiles as waves propagate shoreward. Up to the first breaker bar, the model is able to capture the vertical profiles of undertow. Onshore from the first bar, the model underestimates the vertical mixing which is probably due to the fact that its contribution originates from the breaking-induced turbulence, which is not taken into account in the model.

The wave-averaged turbulence intensity profiles are shown in Fig. 5. Obviously, just after the first bar, turbulence generated in the water surface by wave breaking is clearly underestimated. However, in the trough region, i.e. between 22 m and 25 m, there is no wave breaking and the diffusive transport of the turbulent kinetic energy produced by the roller downward through the water column is expected to be small (see also Fig. 6.4 of Boers (2005)). Hence, the vertical profiles of turbulent energy are quite well predicted in this region. This is also the case after the second breaker bar.

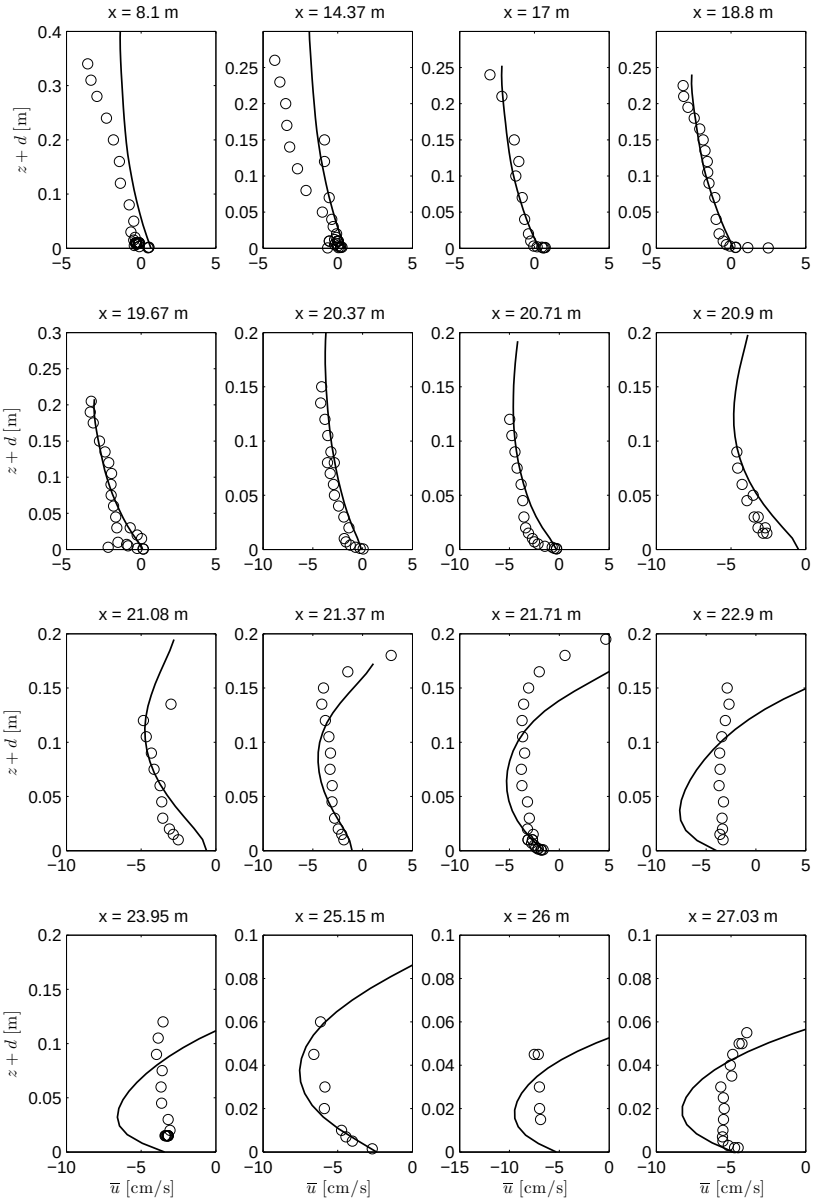

Figure 4: Computed and measured undertow profiles along the flume for Boers 1C. Circles: experimental data; solid line: SWASH.

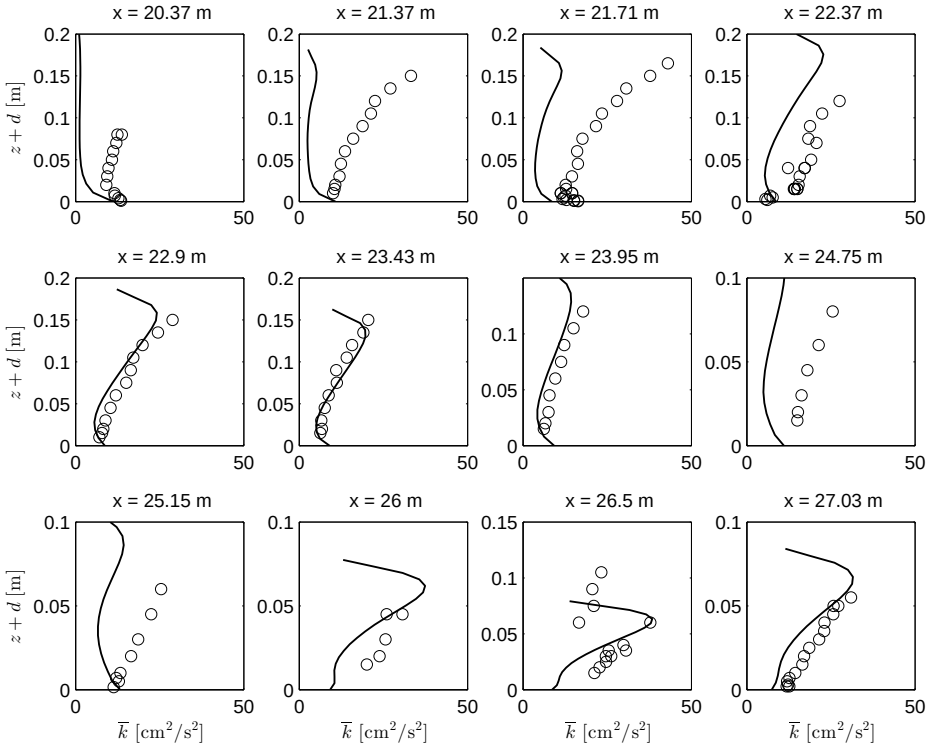

Figure 5: Computed and measured wave-averaged turbulence intensity profiles along the flume for Boers 1C. Circles: experimental data; solid line: SWASH.

Case 1B

The wave field in this case is energetic and has a relatively high mean steepness, and at the wavemaker already has a reasonable amount of energy at superharmonic frequencies.

Fig. 6 depicts the predicted and measured undertow profiles at some cross-shore locations along the flume. In general, close to the bed, velocity profiles are well predicted as turbulence production resulted from mean shear is mainly confined in the bottom boundary layer. However, away from the bed, the profiles are bit more curved. It is believed that this deviation must be attributed to shortcomings in modelling breaking-induced turbulence.

The time-averaged turbulent kinetic energy profiles are shown in Fig. 7. Although the profile shapes are qualitatively similar, these profiles display an underprediction of turbulent energy near the first breaker bar and onshore of the second bar. This reflects the breaking process of which the present lack of modelling production of turbulent energy due to the surface roller is probably the main issue.

CONCLUSIONS

Numerical simulations were undertaken with the non-hydrostatic wave-flow model SWASH to evaluate its ability to describe surf zone hydrodynamics. The following conclusions can be drawn from the comparison between the SWASH results and the laboratory data of Boers (2005).

- Comparison of model predictions with observations of wave height, spectra in surf zone, and wave-induced setup is excellent.
- With the used vertical resolution, i.e. 20 equally distributed layers, the macro-scale effects of wave breaking are very well captured by the model. No tunable parameters nor breaking criterion were needed.
- Comparison of measured and computed profiles of the undertow and wave-averaged turbulent energy agrees well at some cross-shore locations. There is a reasonable agreement between the predicted and measured vertical profiles of the mean horizontal velocity. Also some distance shoreward of the breaker bars vertical mixing is fairly underestimated. Although the turbulence intensities are generally underestimated by the model, the spatial variation and the vertical distribution are captured well by the model.

Based on these comparisons, we can conclude that SWASH can reasonably simulate the surf zone hydrodynamics.

The contribution of wave-generated turbulence to the undertow seems to be important. Therefore, it is recommended to implement the contribution of the surface roller as a turbulence production into the existing $k-\varepsilon$ type models. However, the usual approach is to assume that this production equals the rate of energy dissipation in the surface roller, which is appropriate for phase-averaged wave models. In the context of non-hydrostatic wave-flow modelling suited for the simulation of intra-wave motions, another route is sought. One approach suggested in Reniers et al. (2013) is based on the assumption that wave breaking occur when wave fronts exceed a critical slope. A source term for the intra-wave generation of turbulent energy is proposed that is related to this slope. This method will be implemented in SWASH in the near future.

ACKNOWLEDGEMENTS

Many thanks are due to Marien Boers from Deltares for providing his valuable laboratory data.

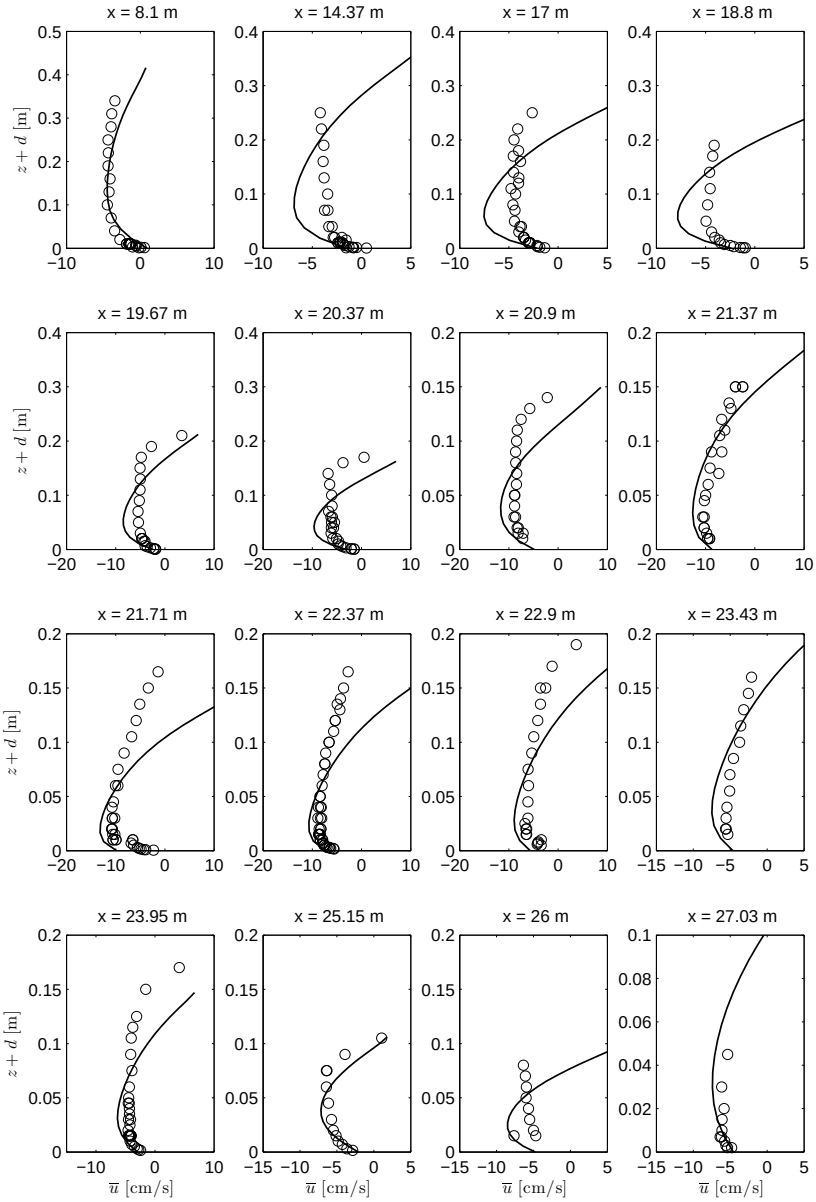

Figure 6: Computed and measured undertow profiles along the flume for Boers 1B. Circles: experimental data; solid line: SWASH.

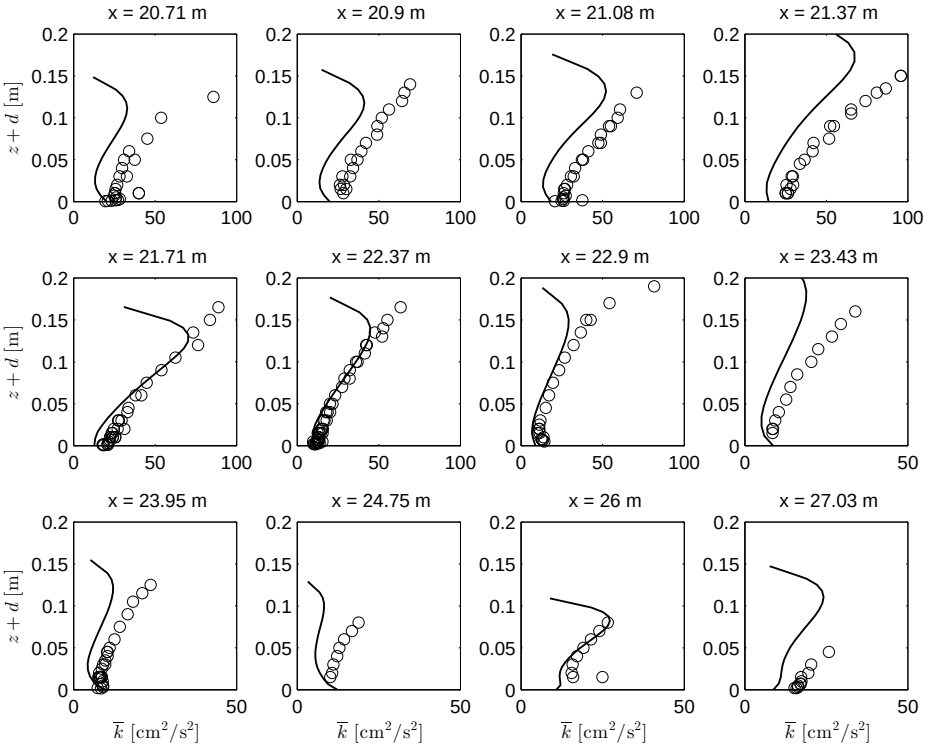

Figure 7: Computed and measured mean turbulence intensity profiles along the flume for Boers 1B. Circles: experimental data; solid line: SWASH.

References

M. Boers. *Surf zone turbulence*. Ph.D. thesis, Delft University of Technology, 2005.

S. Bradford. Numerical simulation of surf zone dynamics. *J. Waterw. Port Coast. Ocean Eng.*, 126:1–13, 2000.

E. Christensen, D.-J. Walstra, and N. Emerat. Vertical variation of the flow across the surf zone. *Coast. Engng.*, 45:169–198, 2002.

B. Launder. Turbulence modeling in the vicinity of a wall. In S. Kline, B. Cantwell, and G. Lilley, editors, *Complex turbulent flows: comparison of computation and experiment*, volume II, pages 691–699, Stanford University Press, Stanford, CA, 1982.

B. Launder and D. Spalding. The numerical computation of turbulent flows. *Comput. Meth. Appl. Mech. Engng.*, 3:269–289, 1974.

P. Lin and P.-F. Liu. A numerical study of breaking waves in the surf zone. *J. Fluid Mech.*, 359:239–264, 1998.

A. J. H. M. Reniers, E. L. Gallagher, J. H. MacMahan, J. A. Brown, A. A. van Rooijen, J. S. M. van Thiel de Vries, and B. C. van Prooijen. Observations and modeling of steep-beach grain-size variability. *J. Geophys. Res. Oceans*, 118:577–591, 2013.

D. Rijnsdorp, P. Smit, and M. Zijlema. Non-hydrostatic modelling of infragravity waves under laboratory conditions. *Coast. Engng.*, 85:30–42, 2014.

G. Stelling and S. Duinmeijer. A staggered conservative scheme for every Froude number in rapidly varied shallow water flows. *Int. J. Numer. Meth. Fluids*, 43:1329–1354, 2003.

J. Van der Werf, K. Neessen, J. Ribberink, and W. Kranenburg. Wave breaking effects on mean surf zone hydrodynamics. In *Coastal Dynamics 2013*, pages 1763–1774, Bordeaux University - SHOM, 2013.

Z. Wang, Q. Zou, and D. Reeve. Simulation of spilling breaking waves using a two phase flow CFD model. *Comput. Fluids*, 38:1995–2005, 2009.

I. Wenneker, A. van Dongeren, J. Lescinski, D. Roelvink, and M. Borsboom. A Boussinesq-type wave driver for a morphodynamical model to predict short-term morphology. *Coast. Engng.*, 58:66–84, 2011.

Q. Zhao, S. Armfield, and K. Tanimoto. Numerical simulation of breaking waves by a multi-scale turbulence model. *Coast. Engng.*, 51:53–80, 2004.

M. Zijlema and G. Stelling. Further experiences with computing non-hydrostatic free-surface flows involving water waves. *Int. J. Numer. Meth. Fluids*, 48:169–197, 2005.

M. Zijlema and G. Stelling. Efficient computation of surf zone waves using the nonlinear shallow water equations with non-hydrostatic pressure. *Coast. Engng.*, 55:780–790, 2008.

M. Zijlema, G. Stelling, and P. Smit. SWASH: an operational public domain code for simulating wave fields and rapidly varied flows in coastal waters. *Coast. Engng.*, 58:992–1012, 2011.